Hindawi
Advances in Materials Science and Engineering
Volume 2020, Article ID 2846721, 11 pages
https://doi.org/10.1155/2020/2846721

Research Article

The Effect of Ageing Treatment on Shape-Setting and Shape Memory Effect of a NiTi SMA Corrugated Structure

Yuanye Zhan,[1] Liang He,[1] Xiaofeng Lu,[1] Xiaolei Zhu,[1] and Qing Chen[2]

[1]*College of Mechanical and Power Engineering, Nanjing Tech University, Nanjing 211800, China*
[2]*College of Mechanical and Electrical Engineering, Jilin Institute of Chemical Technology, Jilin 132022, China*

Correspondence should be addressed to Xiaolei Zhu; zhuxiaolei@njtech.edu.cn

Received 3 April 2020; Revised 22 May 2020; Accepted 1 June 2020; Published 19 June 2020

Academic Editor: Gianfranco Palumbo

Ageing treatments were performed on Ti-50.53 at.% Ni shape memory alloy corrugated gasket (SMA-CG) units. The results of phase transition temperature, shape-setting, compression-resilience performance, and the shape memory effect (SME) of NiTi corrugated units were investigated. The experimental results show that high austenite finish temperatures could be achieved at 500°C and at 400°C aged for a long time, while the martensite finish temperatures were basically above room temperature. The peak value of the austenite finish temperature was found to be 500°C. The shape-setting result was better with the increase of ageing temperature and ageing time. It was stable when units were constrain-treated at 500°C and the ageing time was longer than 30 min. As the strain increases, the resilience rate of the unit decreased rapidly. The resilience rate decreased with the ageing process. Most of the aged units exhibited good SME when the maximum strain was less than 40%. There was the best recoverability when the ageing treatment was performed at 500°C for 60 min.

1. Introduction

In the process industry, it is important for a gasket to adapt to flange irregularities and to any dimensional changes of the flange system caused by temperature changes during operation. Corrugated metal gasket can be used in low pressure applications that require a thin line contact because of space or weight limitations. The unique properties such as shape memory effect (SME) and superelasticity (SE) make NiTi an excellent candidate in the design of corrugated metal gasket [1–4]. However, the complexity of manufacturing and shape setting the SMA structure hinders the widespread use of NiTi alloys. NiTi alloys structures need to be formed or shape-set into desired shapes for practical engineering application. For this purpose, NiTi corrugated units are manufactured using certain heat treatment, commonly an ageing treatment, and are applied to the final product to shape-set and the properties are optimized at room temperature [5].

Efremov [1] first presented a novel type of bolt flange connection (BFC) that contained blots and gasket with cores manufactured from SMA. The combination of SMA of the bolts and gasket excluded the flange rotation and created continuous and leak-tight joint that can extend the safe service life of critical engineering structures. Then, Efremov [2–4] provided the methods to fabricate the corrugated cores of shape memory alloys that displayed the negative creep effect under operating conditions. The corrugated gasket could be manufactured from SMA by using a die-stamp to press the flat sheet of SMA at temperature below the temperature of direct martensitic phase transformation from austenite to martensite of the SMA. Then, it was subjected to continuous ageing at temperature higher than temperature of reverse martensitic phase transformation from martensite to austenite of the SMA before releasing the fixation. But the specific process of shape-setting had not been studied.

Liu et al. [5, 6] optimized the thermal treatment parameters for fixing the NiTi stent wires. The results of NiTi stent shape-setting treatment were evaluated in terms of the angles between the adjacent stent struts. The treated NiTi wires exhibited good recovery ability at body temperature when the short time ageing treatments were performed at

500°C. Elahinia et al. [7] discussed the details in shape-setting of SMA wires in order to attain desired shape memory properties. Heat treating temperatures for binary NiTi alloys are usually chosen in the narrower range of 325–525°C, and heat treating times are typically 5–30 min. Benafan et al. [8] discussed the thermomechanical process employed in creating most SMA actuators. A common practice for shape-setting entails four parts. Firstly, mechanically constraining the fabricated material within a fixture of the desired shape. Secondly, heat treating the constrained material at a high temperature for a dwell time (commonly at 500°C for 1 h for NiTi). Thirdly, cooling the material (vacuum, air, or quenching) and finally optimizing the final geometry through subsequent shape sets or additional machining. Johnson and Alauddin [9] shape-set a shape memory alloy dental arch. They used Joule heating to heat the wire to annealing temperature quickly, then simultaneously quenching and shaping the material, and cooling it very rapidly. That allowed the single crystal material to be shape-set without diminishing the material properties.

Ageing or annealing of the SMA subsequent to the shape-setting operation is one way to change the material properties of the SMA including the yield strengths and the phase transformation temperature. Most SMA components like wires and tubes are shape-set annealed condition [10]. For Ni-rich alloys, applying ageing treatment leads to dispersing Ni_4Ti_3 precipitates in the matrix. These precipitates change the transformation sequences of the alloy [11, 12]. There is only a specific temperature and time of ageing that can produce coherent Ni_4Ti_3 precipitates that are useful for improving shape memory behavior of the alloy [13]. Kim and Miyazaki [14] clarified the effect of low temperature ageing (<327°C) on the shape memory behavior of a Ti-50.9 at.% Ni alloy. According to their results, the size of Ni_4Ti_3 precipitates hardly increases, but their density increases with increasing ageing time. Fine and dense Ni_4Ti_3 precipitates act as effective obstacles against the movement of dislocations. As the precipitates grow larger with increasing ageing temperature and time, the maximum recovery strain decreases. Jiang et al. [13] found that the sample aged at 450°C resulted in fine and dense Ni_4Ti_3 precipitates and showed the highest yield strength. Pelton et al. [15] found that the transformation temperature, and hence the properties, could be accurately tuned by selective ageing treatments. Higher A_f temperatures were achieved by ageing in the 300–500°C range. Yeung et al. [16] explored the effect of heat treatment on the transformation characteristics to the austenite phase. The specimens were aged at 200–400°C for 30–60 min, respectively. They found that the austenite phase transition temperature can be manipulated by varying the heat treatment parameters such as ageing time, heat treatment temperature, and cooling rate. Heat treatment temperature was the most critical factor to change the austenitic phase transition temperature. Razali and Mahmud [17] focused on the sensitivity of critical stress needed for stress-induced martensitic transformation over different ageing temperatures. He found that the suitable temperature range for creating a gradient stress plateau of stress-induced martensite transformation of Ti-50.8 at.% Ni was between 400 and 500°C. Aboutalebi et al. [18] evaluated the ageing treatments on the phase transformation and superelasticity of Ti-51.5 at.% Ni. For the aged samples, complete superelasticity was observed by ageing at 400 and 500°C. Favier et al. [19] investigated that the influences on the transformation and mechanical behavior of NiTi were greater for constrained ageing than for free ageing because the applied stress will encourage the formation of precipitates preferentially aligned with the external tensile stress, perpendicular to the external compressive stress, to relax the internal stresses.

However, there were studies on the constrained ageing treatment of nitinol wires in the medical neighbourhood. And the lowest martensite phase transition temperature of the binary NiTi alloy currently studied was mostly below room temperature. It limited the temperature range to manufacturing SMA gasket. Knowledge of the shape-setting treatment parameters appropriate to the applications in corrugated gaskets and in the field of sealing is far from sufficient. In this study, our focus was to optimize the ageing treatment parameters for fixing the NiTi corrugated gasket unit to achieve the best result of shape-setting. It could be applied to the manufacture of shape memory alloy corrugated gasket. Simultaneously, the unit was expected to be provided with great compression-resilience rate and shape-recovering ability. It could remain in martensitic state at room temperature in all normal condition of use.

2. Experimental

The material used in this study was Ti-55.59 wt.% Ni (Ti-50.53 at.% Ni) shape memory alloy sheet metal with a thickness of 0.3 mm. The corresponding chemical composition is given in Table 1. The phase transition temperatures (M_f, M_s, A_s, and A_f) of the as-received specimen were 19.48, 54.58, 51.20, and 76.50°C. The schematic diagram of a shape memory alloy corrugated gasket (SMA-CG) and a SMA-CG unit is shown in Figure 1.

Nitinol sheets were constrained to the shape of a SMA-CG unit on a shape-setting mold. The mold is shown in Figure 2. Shape-set ageing treatments were performed on the sheets, together with the molds, at temperatures of 300, 400, and 500°C for 10, 30, and 60 min in a tube furnace (BTF-1400C, China), followed by air cooling. To minimize the oxidation of the samples at high temperatures, high purity Argon gas (99.99% Ar) was purged into the furnace chamber during treatment. Flat thin specimens of 10 mm length taken from the same sheets were aged in the same furnace for phase transformation and metallography tests [5].

The phase transformation temperatures were measured by differential scanning calorimetry (DSC) using a Diamond DSC Pyris 1 instrument with a liquid nitrogen cooling accessory. The weight of specimens was between 10 and 20 mg. The heating and cooling regime was as follows: specimens were heated up quickly to 150°C and kept isothermal for 5 min, cooled down to 0°C, and also kept isothermal for 5 min and then heated to 150°C again. Cooling and heating rate during thermal cycling was 10°C/min.

Table 1: Chemical composition of NiTi (wt.%).

Ni	Co	Cu	Cr	Fe	Nb	C	H	O	N	Ti
55.59	0.005	0.005	0.005	0.012	0.005	0.046	0.001	0.03	0.001	Margin

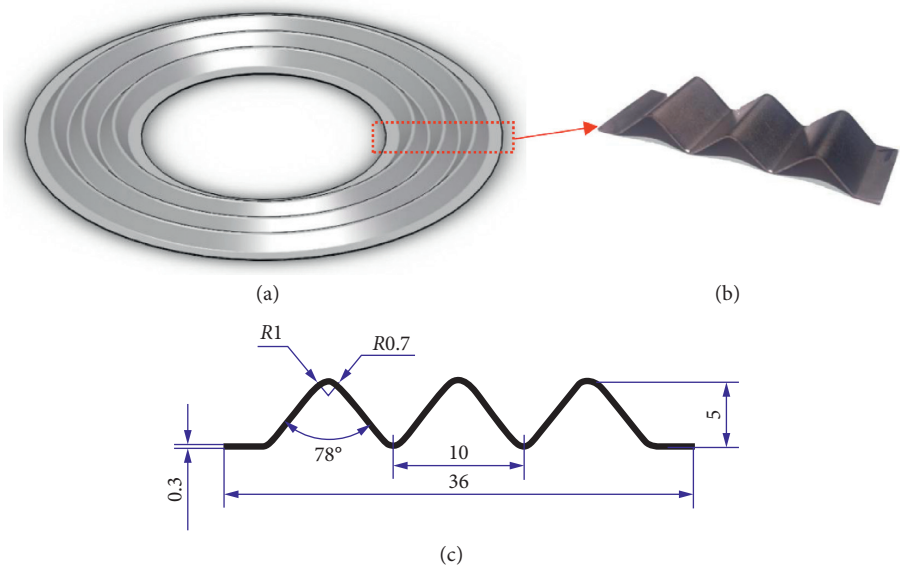

Figure 1: Schematic diagram of SMA-CG and SMA-CG unit: (a) SMA-CG; (b) one unit of the SMA-CG; and (c) expected dimensions of the unit.

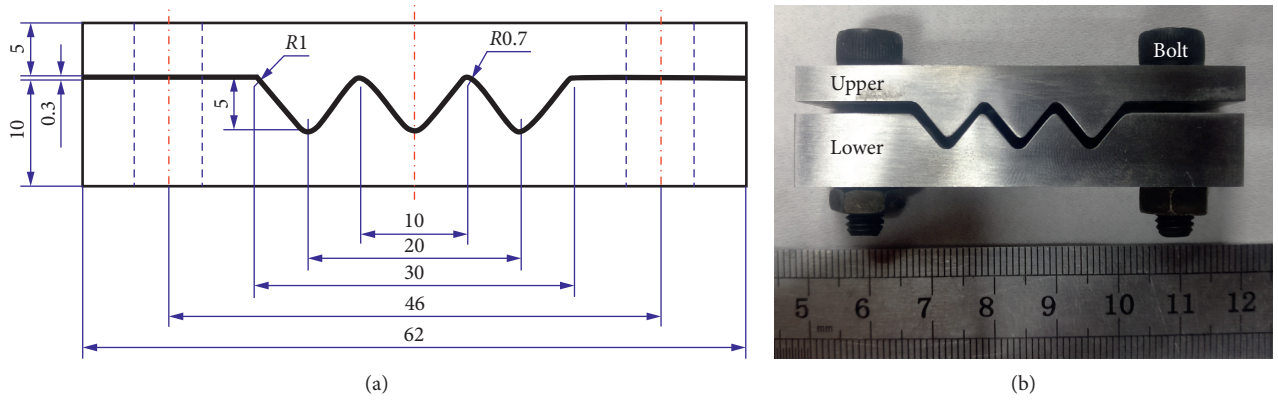

Figure 2: Shape-setting mold: (a) Dimensions of the mold; (b) mold assembly.

NiTi alloy is more sensitive to temperature. Epoxide resin and curing agent were used for cold mounting. Metallographic specimens were ground on silicon carbide papers and then polished. The microstructure was examined by optical microscopy (OLYMPUS-DSX510) after etching with diluted solution (10 vol. % HF + 40 vol. % HNO_3 + 50 vol. % H_2O) at room temperature (RT) [20].

The angles θ between the adjacent struts of corrugates were used to evaluate the results of the shape-setting. The stereo microscope (OLYMPUS-SZX10, Japan) was used to measure the angles θ in order to ensure accuracy. The instrument and the example of measurement are shown in Figure 3. The angles after shape-set ageing treatments were recorded as angle θ_1. Then the SMA-CG units were reheated to the austenite finish temperature ($T \geq A_f$) using a resistance furnace. The angle θ_2 was recorded. The reheating temperature was 100°C.

Since the stress-strain curve is sensitive to the test temperature, all compression-resilience tests were performed at room temperature (25°C) on an Instron 3367 desktop electronic testing machine. To minimize the thermal effect associated with the phase transition on the mechanical properties, all compression-resilience tests were conducted at a strain rate of $2.0 \times 10^{-4}\,s^{-1}$ [21]. In these tests, SMA-CG units were compressed to the maximum strain and unloaded to zero stress at room temperature. All experiments were carried out under strain controlled with different fixed maximum strains (20, 30, 40, 50, 70, and 100%). The

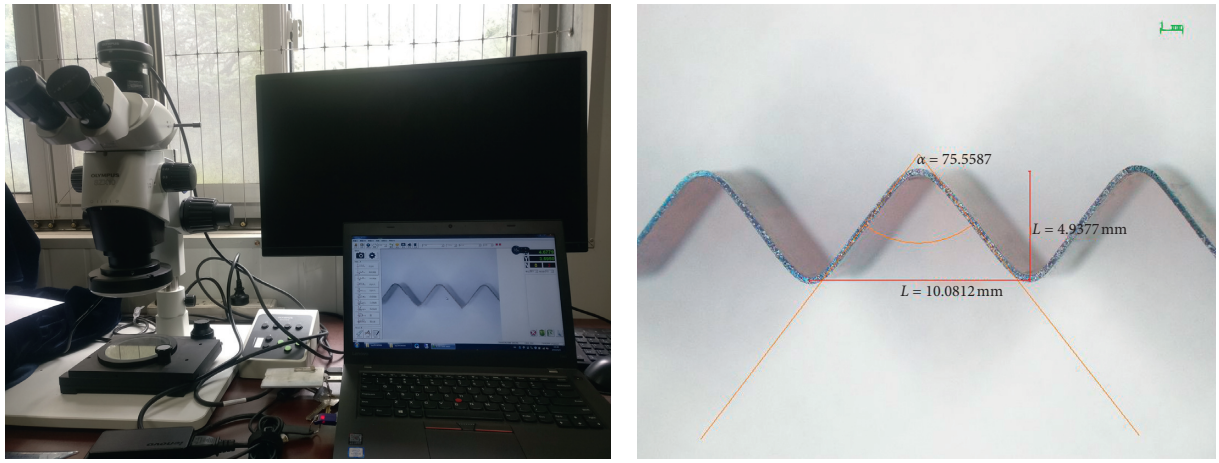

(a) (b)

Figure 3: The measurement of angle θ: (a) OLYMUPS-SZX10; (b) one example of measurement result.

maximum strains were calculated and controlled based on the macro height of the corrugated unit. Compression-resilience performance can be evaluated using resilience rate. It can be characterized by the change of the angle. The equation is expressed as follows:

$$\text{resilience rate } (\%) = \left(1 - \frac{\theta_{2n} - \theta_2}{\theta_2}\right) \times 100, \quad (1)$$

where θ_2 is the initial angle recorded after warming in free state and θ_{2n} is the angle recorded after the compression and resilience.

After the compression-resilience tests, reheat the SMA-CG units above the austenite finish temperature ($T > A_f$) using a resistance furnace. The reheating temperature is 100°C. Characterize the shape memory effect (SME) of SMA-CG units after loading by measuring the angles θ and calculating the recovery rates Δ. The equation representing the recovery rate Δ can be expressed as follows:

$$\Delta\ (\%) = \left(1 - \frac{\theta_3 - \theta_2}{\theta_2}\right) \times 100, \quad (2)$$

where θ_3 is the angle of warming after the compression-resilience tests. The schematic diagram of shape memory effect is shown in Figure 4. It shows the changes in the state of the sample during the tests. When the unit was compressed, there was residual deformation and it could not fully rebound. After reheating, the corrugated unit tended to return to its original shape.

3. Results

3.1. Correlations between the Transition Temperatures and Ageing Treatment. Figure 5 shows typical DSC curves of specimens aged at various temperatures for different times. The peaks of phase transformation were completely obvious and sharp after ageing. In the DSC curve, when the specimen was cooling down, M_s and M_f were defined as martensite phase transition start and finish temperature, respectively. While the specimen was heated up, A_s and A_f were defined as austenite phase transition start and finish temperature, respectively. The hysteresis (A_s–M_s) can be measured by taking the temperature different between the forward and reverse transformation. For the samples heat-treated at 300 and 400°C, the DSC thermograms show a single-stage transformations, forward ($A^\circ \longrightarrow {}^\circ M$) and reverse ($M^\circ \longrightarrow {}^\circ A$). The R phase was obvious when samples were heat-treated at 500°C. ($M^\circ \longrightarrow {}^\circ A$) and ($R^\circ \longrightarrow {}^\circ A$) peaks could be recognized easily by increasing ageing temperature to 500°C. For the Ni-rich NiTi, the R phase was present during heating processes, below the recrystallization temperature. Figures 6(a)–6(d) show the effects of heat treatment temperature and time on M_f, M_s, A_s, and A_f temperature. As seen in Figure 6(a), the M_f temperature increased after the ageing treatment. Aged at 300°C, the temperature increase was smaller than that at 400 and 500°C. It was found that the temperatures changed little over ageing time. As seen in Figure 6(b), M_s increased with ageing temperature. It increased only slightly with ageing time at 400 and 500°C, while it was opposite at 300°C. Overall, the temperatures were lower than the original sample. The changes of A_s are shown in Figure 6(c), which were basically consistent with the changes of M_f. As seen in Figure 6(d), the A_f temperatures decreased with ageing time at 150°C. At 400°C, there was an initial decrease in A_f and then a rapid increase. At the highest ageing temperature, 500°C, the A_f temperature changed significantly and was higher than that processed at 300 and 400°C. It increased with ageing time and reached a maximum of 79.4°C at 60 min. Figure 6(e) shows the effects of ageing temperature and time on transformation hysteresis (A_s–M_s). The (A_s–M_s) temperatures all increased after the ageing treatment. It was found that there was an initial increase in (A_s–M_s) and then a rapid decrease at 300 and 400°C. There was a maximum phase transformation hysteresis at 400°C for 30 min. The transformation hysteresis changed only modestly with ageing time at 500°C, and the value was slightly lower than that at 300 and 400°C.

The optical micrographs presented in Figure 7 show clearly the martensite, grain boundaries, and the presence of

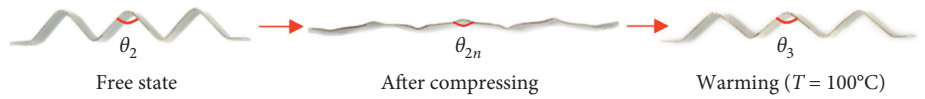

Figure 4: Schematic diagram of the shape memory effect of SMA-CG unit.

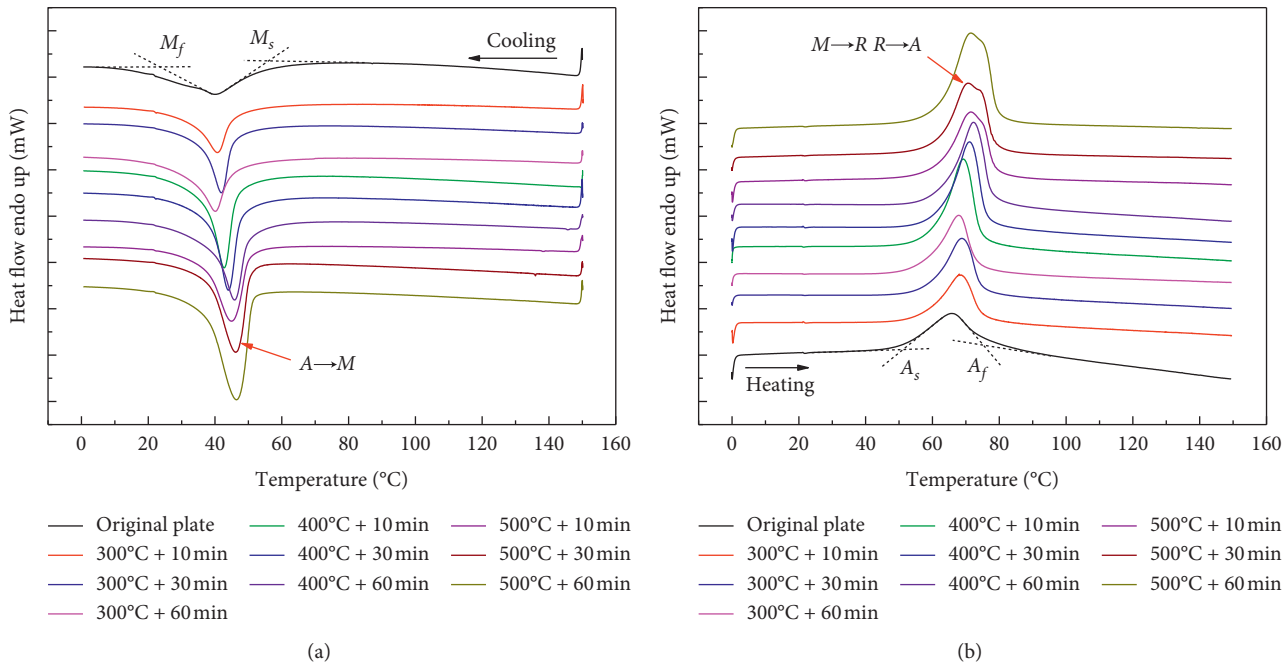

Figure 5: DSC curves of the samples after thermomechanical treatment: (a) Cooling; (b) heating.

particles with different sizes. The matrix structure observed at room temperature was mainly martensite, with a small amount of austenite. The density of these particles seems to be higher in the 500°C aged sample than that of the 300 and 400°C aged sample. There are larger uniform coherent precipitates [22].

3.2. Correlations between the Results of Shape-Setting and Ageing Treatment. The geometries of the SMA-CG unit have a strong relationship with ageing temperature and time. Figure 8 shows the physical diagram of the units after ageing treatment at different temperatures for 10 min. Angles θ_1 and θ_2 represented the angles before and after warming in the free state, respectively.

The results and comparison of angles θ_1 and θ_2 are shown in Figure 9. Common cold stamping without shape-setting treatment could not prepare the SMA-CG unit and the angle θ_1 was 105.5°. As seen in Figure 9(a), the angles θ_1 of the units after different shape-setting treatments were basically the same. They got close to 76.5° and the difference between the maximum and minimum was 1.42°. As seen in Figure 9(b), the angles θ tended to increase after warmed above the austenite finish temperature (T = 100°C). Ageing treatments did not set the shape of the units absolutely. When the ageing treatment was performed at 300 and 400°C for longer time, the angles θ_2 got smaller. The angles changed only modestly at 500°C for 30 to 60 min. As seen in Figure 9(c), there was poor shape maintenance at 300°C even for longer time. The maximum angle θ_2 was 84.37° and the maximum increment compared to angle θ_1 was 8.08°. The angle was maintained better after 400°C for 60 min and the increment was 1.95°. At the highest ageing temperature, 500°C, the shape maintenance worked best and the increments were less than 1°.

3.3. Correlations between the Mechanical Properties and Ageing Treatment. Figure 10 is the summary plot of the resilience rate for SMA-CG units after loading. The figure shows that the resilience rate of the corrugated unit decreased with strain (20–100%). The trends were basically the same when aged at different treatment temperatures for 10 to 60 min. When the strain was less than 70%, there was the highest resilience rate at 300°C, it decreased slightly with ageing temperature. There was rapid decreased in resilience rate as temperature rising; it was most obvious at 500°C. When the strain was 40%, the resilience rate decreased below 25%, and then the trend slowed down. The rates were basically the same under the final strain, 100%. The final rates got closer to 20%.

3.4. Correlations between the Shape Memory Effect and Ageing Treatment. The recovery rate Δ was discussed to characterize the shape memory effect of SMA-CG units. It was

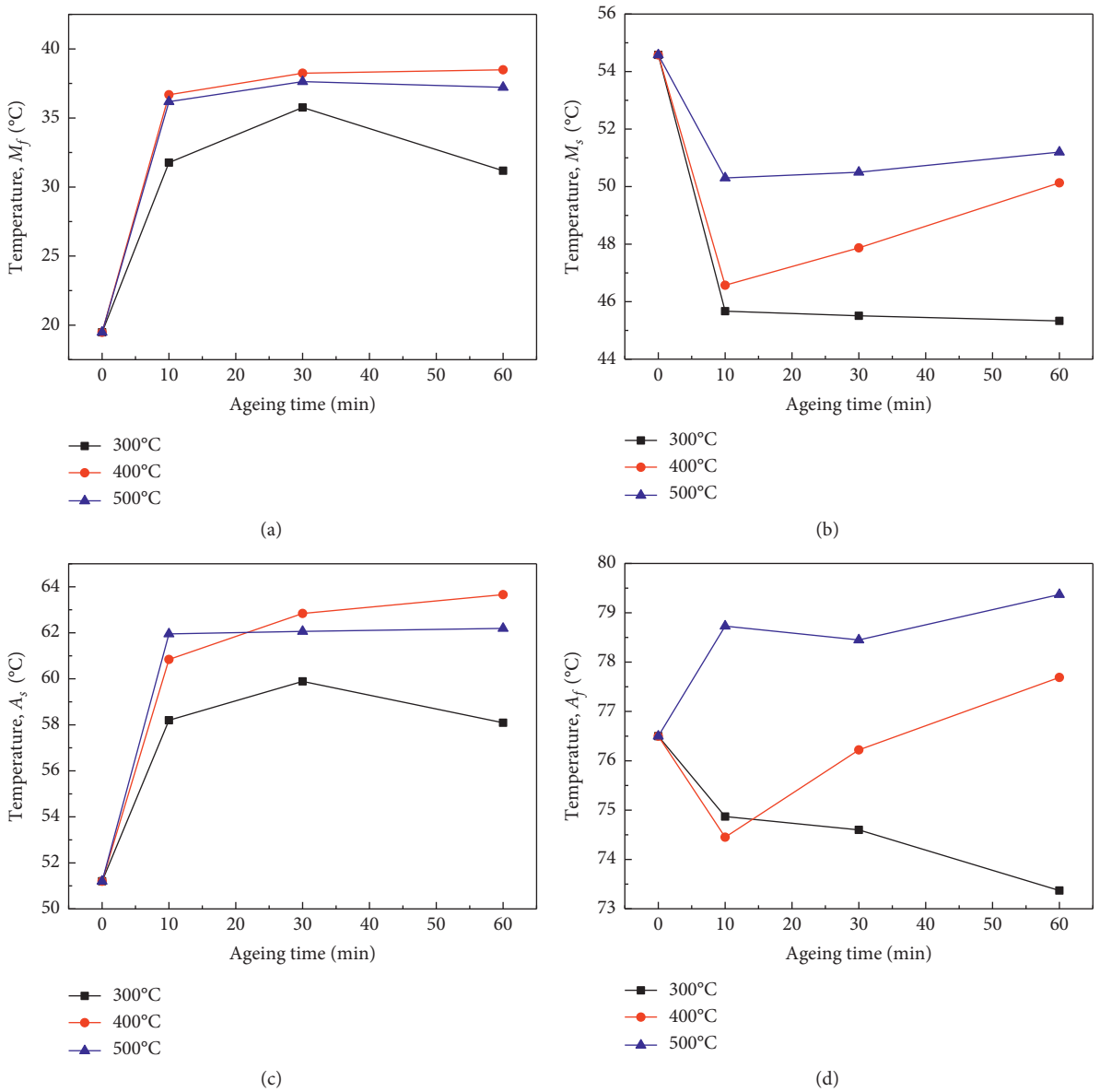

Figure 6: Continued.

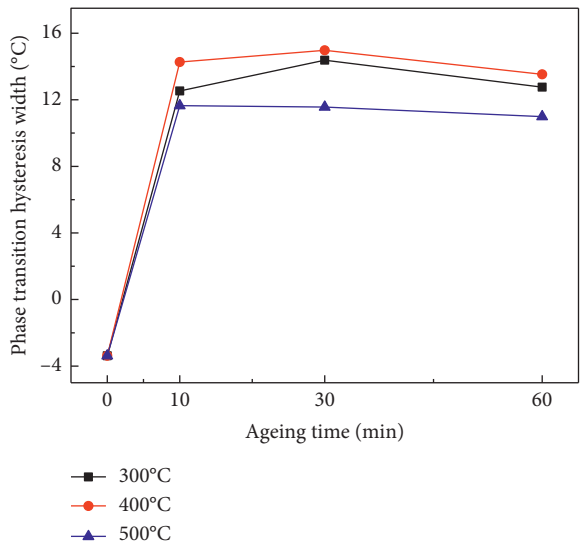

(e)

Figure 6: Effect of ageing treatment on phase temperature: (a) martensite phase transition finish temperature M_f; (b) martensite phase transition start temperature M_s; (c) austenite phase transition start temperature A_s; (d) austenite phase finish temperature A_f; (e) effect of ageing treatment on transformation hysteresis (A_s–M_s).

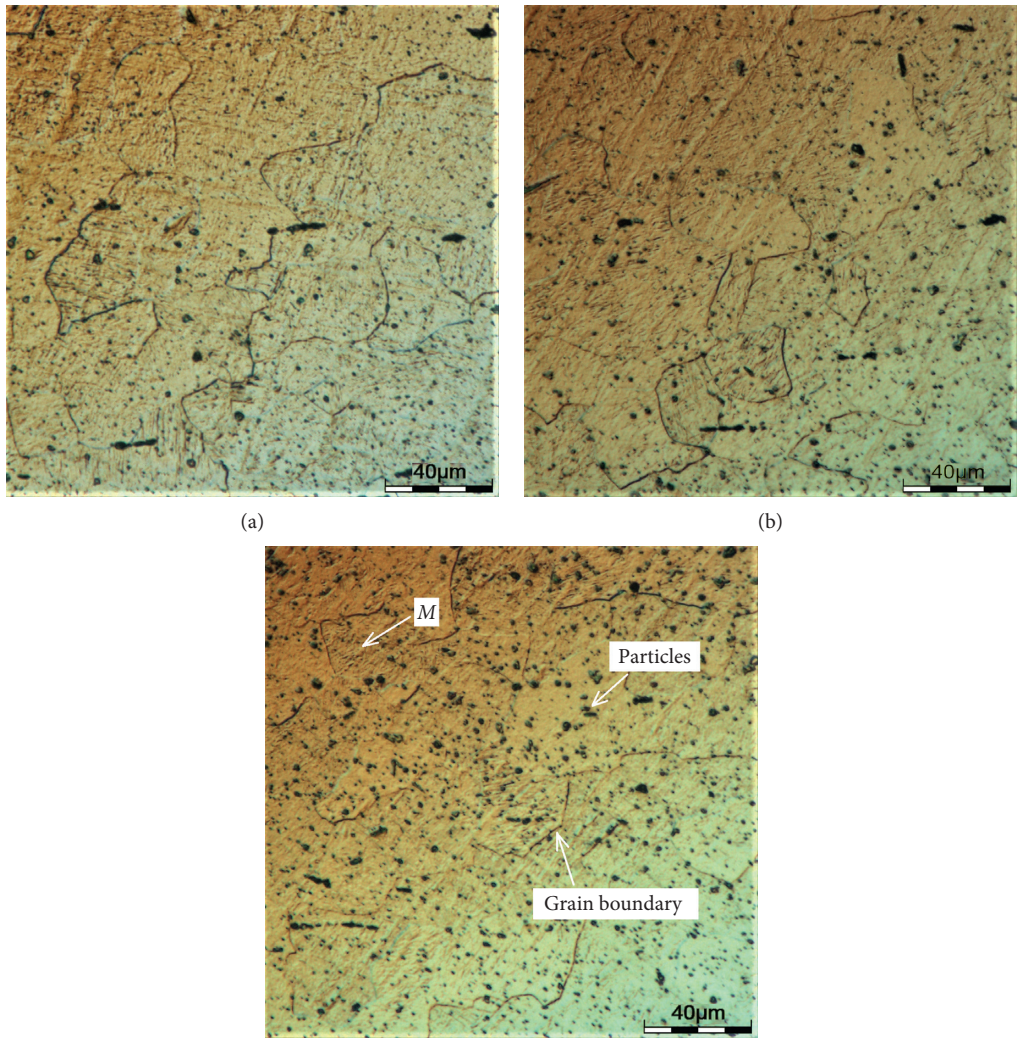

(a) (b)

(c)

Figure 7: Optical micrographs of specimens heat-treated at (a) 300°C; (b) 400°C; and (c) 500°C for 10 min.

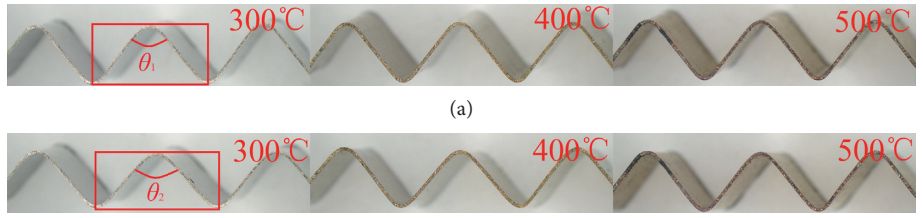

FIGURE 8: Physical diagram of units after ageing treatment at different temperatures for 10 min: (a) Completing the initial shape-set ageing treatment; (b) after warming in the free state ($T = 100^{\circ}C$).

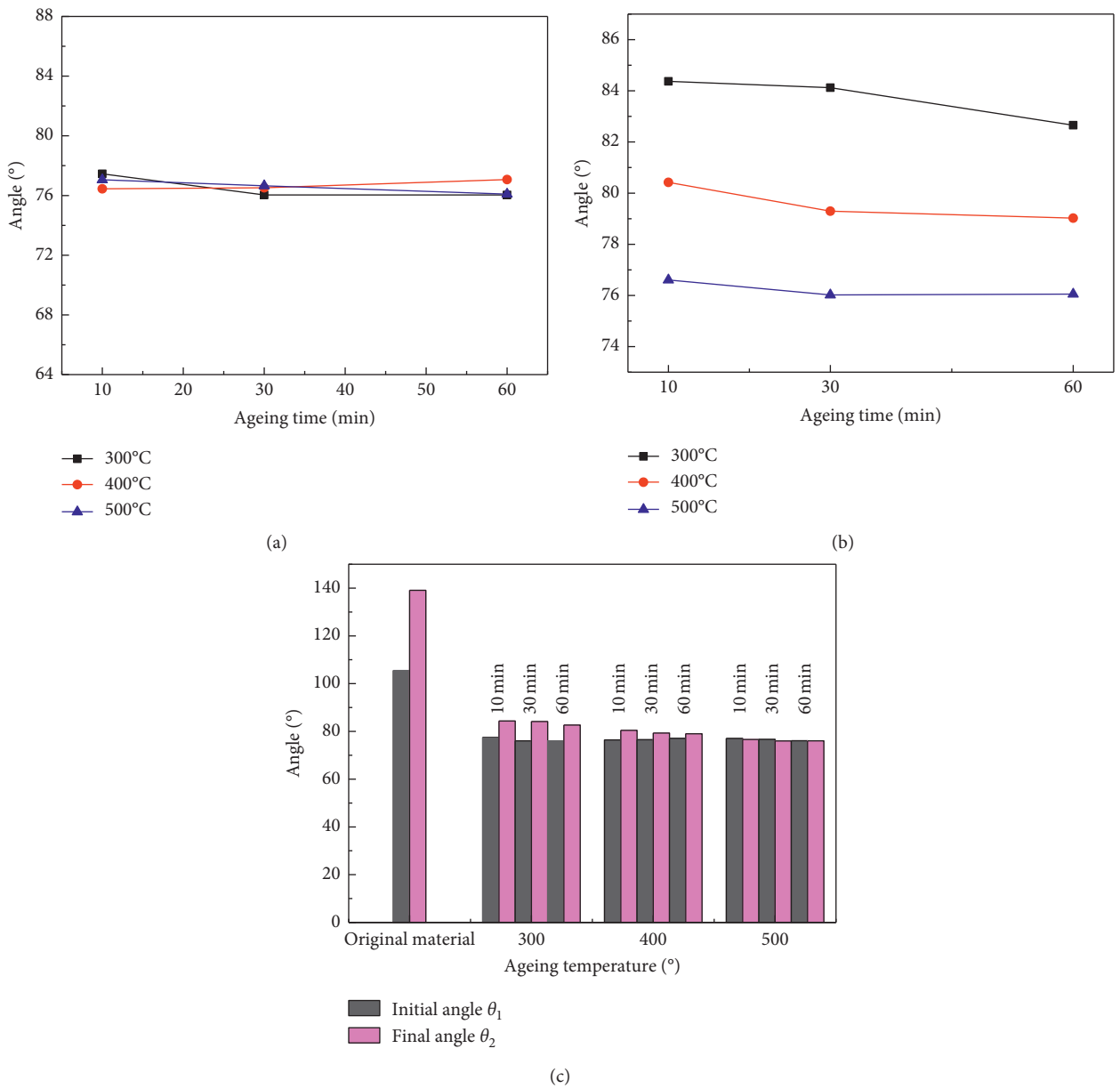

FIGURE 9: Results and comparison of angles θ between the adjacent unit struts: (a) Angles θ_1; (b) angles θ_2; (c) comparison before and after warming up in a free state.

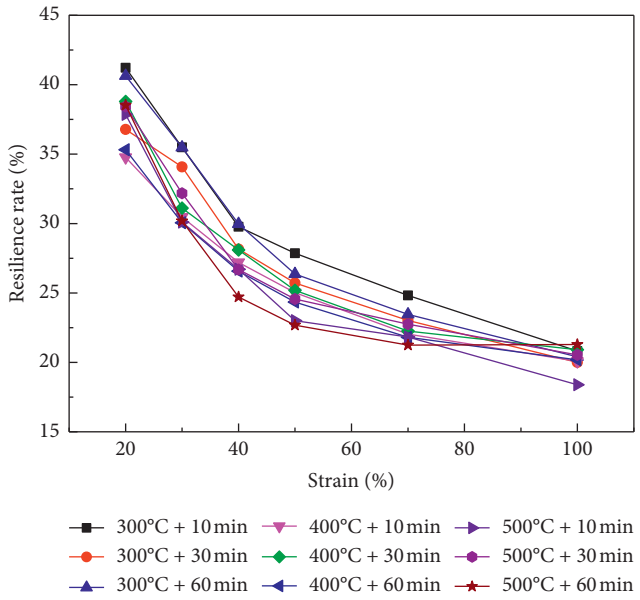

Figure 10: Resilience rates for SMA-CG units after different shape-setting heat treatments.

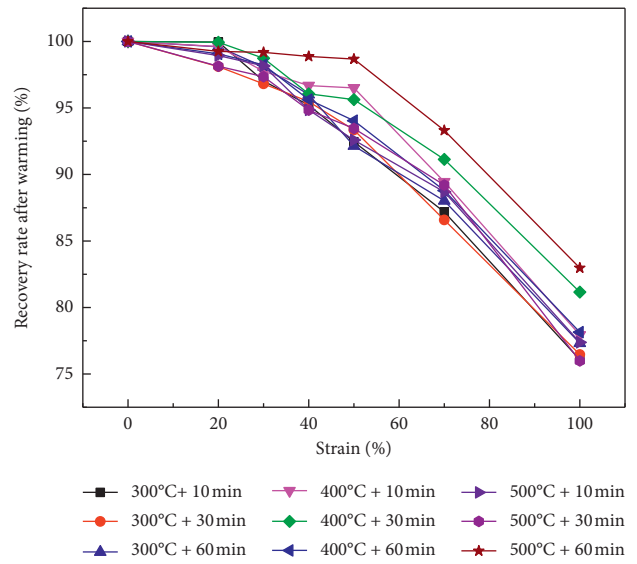

Figure 11: SME of SMA-CG units under different shape-setting treatments after being loaded.

calculated after different ageing treatments and strains. Figure 11 shows the changes in recovery rates in all cases. As seen in Figure 11, all the recovery rates Δ decreased with strain. It represented the reduction of shape memory effect. When the maximum strain was 20%, the recovery rates were over 98%. It was found that the SME changed only modestly with ageing time at 300°C. The final recovery rate was in the range of 76.08% to 77.32%. At 400°C, there was the same recovery rate for different ageing times when the maximum strain was less than 40%. If the strain was over 40%, there was higher recovery rate during short time treatment at 400°C. The final recovery rate was in the range of 77.93% to 81.15% at 400°C. At the highest temperature, 500°C, the ageing time had a greater impact on recovery rate of SMA-CG units. The SME was maintained the best when aged at 500°C for 60 min. The recovery rate was up to 98% when the maximum strain was 20%. At 500°C, the final recovery rate was in the range of 77.38% to 82.97%.

4. Discussion

The phase transition peaks got sharper in the DSC curves. They indicated that the phase transition was obvious after ageing. The defects and internal stresses formed during cold working prevented the motion of interfaces of martensite. As the material is aged, diffusion in the structure of material leads to the annihilation of defects [23].

Shape-setting treatments not only can make the nitinol sheets assume the preferred shape, but also can control the transition temperatures precisely and mechanical performances of the structure. It is known that the metastable Ti_3Ni_4 precipitates affect the phase transition temperatures in Ni-rich NiTi shape memory alloy [11, 22, 24]. The Ni content in the precipitated Ti_3Ni_4 phase changes, which causes a change in the transition temperature. There was an initial decrease in M_s and then an increase. M_f and A_s had an initial increase and then a decrease at 300°C. M_s decreased at 300°C and increased volatility at 400–500°C. After ageing at low temperature (300°C), the NiTi matrix tissue precipitates hardly increase. However, coherent Ni-rich compound will precipitate over time, which is not conductive to martensitic transformation [14]. The peak values of A_f temperatures were obtained after ageing at high temperature, 500°C. These effects can be understood by briefly exploring two factors that control the nucleation and growth of precipitates. At high temperatures, there is sufficient thermal energy to permit rapid diffusion of Ni and Ti atoms in the matrix. Ni atoms gather in the precipitates and Ti atoms move to the TiNi matrix phase. The DSC thermogram corresponding to the temperature of 500°C reveals multistage transformations ($M^\circ \longrightarrow {}^\circ R\ R^\circ \longrightarrow {}^\circ A$) which indicate the formation of uniformly distributed coherent Ni_4Ti_3 precipitates. Local composition changes will affect the transition temperature although the overall composition is still Ti-50.53 at.% Ni. Pelton et al. [15] obtained the maximum A_f in the reaction at about 425°C. His research explained this phenomenon. At lower temperatures, higher nucleation rates will occur, but the diffusion rates will be lower. These two processes are balanced at the temperatures (350–450°C) to achieve maximum precipitation rates. The original specimen in this paper is 0.27 at.% Ni less than Pelton's. We saw the peak values of A_f at 500°C. If the temperature exceeds 500°C, the precipitates will dissolve. And the transition temperature will decrease as the Ni atoms diffuse back in the matrix [25].

The dual-state temperature characteristics of NiTi SMA are temperature-lagging. The transformation hysteresis (A_s–M_s) is related to thermal-mechanical treatment, processing method, and ternary element. There was large phase transformation hysteresis (A_s–M_s) after ageing at 300 and 400°C for short time. The transformation hysteresis changed only modestly at 500°C. At 400–500°C, both A_s and M_s

increase. A_s increases because of the releasing of lattice distortion energy during ageing treatment. The orderly structure makes the martensite less elastic strain energy accumulated during the deformation process. It requires more energy for its transformation to the parent phase. M_s increases because of the ordering of crystals during ageing treatment. That reduces the resistance of transforming to the martensitic phase caused by structural defects [16]. In summary, phase transformation temperatures can be easily adjusted by different ageing times and temperatures. Higher A_f temperature can be achieved when ageing at 400–500°C for a long time. In addition, A_f decreased by ageing at 300–400°C for a short time, but the value of phase transition hysteresis (A_s–M_s) can be significantly increased.

SMA gaskets with corrugated structural unit are used under the operating condition of high temperature and undulating load. It is expected to be pretensioned at room temperature ($T < M_f$) and work at higher temperatures ($T > A_f$). It consists in use of reactive shape-recovering stresses generated by deformed corrugation while with recovery of its initial shape. The reactive shape-recovering stresses provide leak-tight, automatic, and continuous contact between flange surfaces [3]. In practical applications, transformation hysteresis (A_s–M_s) ensures that the temperature is still above the martensite phase transition start temperature ($T > M_s$) as much as possible when the operating temperature fluctuates. And the gasket is maintained in a single-phase austenite state without martensitic transformation. Therefore, the ageing treatment at 500°C for long time should be set to achieve a high working temperature A_f, when the installation temperature M_f remains at room temperature.

The result of the shape-setting studies performed here reveals that ageing temperature is the most crucial factor to shape-setting (see Figure 9). Ageing time has little effect on the shape-setting. The nitinol sheets were constrained on the corrugate structure mold. Ageing treatments under this condition created the free ageing condition for the straight sections and the constrained ageing condition for the bent part of the units. The ageing temperature should be higher than 400°C to relieve the stresses and cause the nitinol sheets to retain the shape of SMA-CG units when they were removed from the mold [5]. It can ensure that there is little tendency to return to the sheet after repeated heating; that is, the ability to maintain its structure is great. The shape-setting results were stable when the NiTi corrugated units were constrain-treated on the mold at 500°C for ageing time longer than 30 min. At the temperature 500°C for ageing time 30–60 min, the shape maintenance worked best.

The resilience rate of SMA-CG unit decreased with maximum strain. The resilience rate decreased faster with increasing ageing temperature. As seen in Figure 10, the resilience rate dropped below 25% when the strain was 40%. Ti_3Ni_4 and $Ti_{11}Ni_{14}$ phase are easily precipitated at the early stage of ageing treatment. These sedimentary phases hinder the movement of dislocations. The increase in dislocation resistance leads to an increase of strength and critical stress slip of the matrix. The fine precipitates are coherent with the matrix. With ageing temperature and time increasing, the size of the precipitated phases increases, the coherence decreases, the dislocation resistance decreases, and the strengthening effect on the matrix weakens. This is consistent with the effect of ageing treatment on phase transition temperature. In the initial stage of the ageing, there are many dislocations and substructures remaining in the matrix, resulting in high matrix strength. Therefore, it is easy to obtain great superelasticity at low treatment temperature for a short time. In contrast, the superelasticity and recoverability decreases [26, 27]. It can be seen in Figure 10, for the same maximum strain, that the resilience rate of corrugated unit aged at 300°C was higher than that aged at 400 and 500°C.

The shape memory effect (SME) of SMA-CG is characterized as the recoverability obtained by measuring the changes of angles θ. There was maximum recoverability when the 60 min ageing treatment was performed at 500°C. The strain should be controlled not more than 40% in order to maintain good SME. As for the SME of NiTi alloy, there are high dislocation density and material strength in the parent phase after ageing at low temperatures. Stress-induced martensite reorientation is difficult to occur, which leads to poor shape memory effect. As the ageing temperature rises, the dislocation density in the parent phase decreases, and the parent phase strength decreases. During subsequent deformation, stress-induced martensite reorientation and dislocations are prone to change the internal stresses in the sample [28]. The progressive development of precipitated phases is associated with ageing temperatures in quantity when ageing at 300–500°C. The flaky Ti_3Ni_4 phase particles strengthen the parent phase and preferentially orienting the martensite modification in the sample. Under the combined action of applied stress and coherent stress field around the Ti_3Ni_4 phase, the martensitic variant is easy to choose the preferred orientation that improves the one-way reversible strain [18].

5. Conclusion

In this paper, constrained ageing treatment of NiTi corrugated unit was studied. The results of phase transition temperature, shape-setting, compression-resilience properties, and shape memory effect were investigated. It is observed that transformation peaks get sharper by increasing the ageing temperature and time. Higher A_f temperatures can be achieved at 500°C and at 400°C aged for a long ageing time, while M_f temperatures are above room temperature. The peak values were obtained after ageing at 500°C. The results show that the suitable shape-setting temperature should be chosen at 500°C for NiTi corrugated units. The shape-setting results and ability of maintaining the shape were stable when the units were constrain-treated at 500°C for ageing time longer than 30 min. The resilience rate of the SMA-CG unit decreased with increasing strain. The resilience rate decreased faster as the ageing temperature increased. It decreased the fastest with the increase of strain at 500°C aged for long time. Most of the aged units exhibited good shape memory effect when the maximum strain was less than 40%. 500°C was the optimal ageing temperature for

producing the expected corrugated units. The maximal recoverability could be retained aged at 500°C for 60 min.

Data Availability

The data used to support the findings of this study are available from the corresponding author upon request.

Conflicts of Interest

The authors declare that there are no conflicts of interest regarding the publication of this paper.

Acknowledgments

This work was financially supported by the National Natural Science Foundation of China (Grant no. 11772147).

References

[1] A. Efremov, "Bolted flanged connection for critical engineering applications," in *Proceedings of the ASME 2006 Pressure Vessels and Piping/ICPVT-11 Conference*, vol. 2, Computer Technology, Vancouver, Canada, pp. 103–110, July 2006.

[2] A. Efremov, *High Temperature Negative Creep Gasket and Manufacturing Same*, United State Patent, Alexandria, VA, USA, 2009.

[3] A. Efremov, *Negative Creep Corrugated Gasket and Methods of Manufacturing Same*, United State Patent, Alexandria, VA, USA, 2012.

[4] A. Efremov, *Negative Creep Gasket with Core of Shape Memory Alloy*, United State Patent, Alexandria, VA, USA, 2007.

[5] X. Liu, Y. Wang, D. Yang, and M. Qi, "The effect of ageing treatment on shape-setting and superelasticity of a nitinol stent," *Materials Characterization*, vol. 59, no. 4, pp. 402–406, 2008.

[6] X. Liu, Y. Wang, M. Qi, and D. Yang, "Effects of heat treatment on shape-setting and non-linear mechanical properties of Nitinol stent," *International Conference on Smart Materials and Nanotechnology in Engineering*, vol. 64237 pages, 2007.

[7] M. H. Elahinia, M. Hashemi, M. Tabesh, and S. B. Bhaduri, "Manufacturing and processing of NiTi implants: a review," *Progress in Materials Science*, vol. 57, no. 5, pp. 911–946, 2012.

[8] O. Benafan, J. Brown, and F. T. Calkins, "Shape memory alloy actuator design: CASMART collaborative best practices and case studies," *International Journal of Mechanics and Materials in Design*, vol. 10, no. 1, pp. 1–42, 2014.

[9] A. D. Johnson and S. S. Alauddin, *Shape Setting a Shape Memory Alloy Dental Arch*, United State Patent, Alexandria, VA, USA, 2014.

[10] A. Rao, A. R. Srinivasa, and J. N. Reddy, "Manufacturing and post treatment of SMA Components," in *Design of Shape Memory Alloy (SMA) Actuators*, Springer, Cham, Switzerland, 2015.

[11] J. Khalil-Allafi, A. Dlouhy, and G. Eggeler, "Ni_4Ti_3-precipitation during aging of NiTi shape memory alloys and its influence on martensitic phase transformations," *Acta Materialia*, vol. 50, no. 17, pp. 4255–4274, 2002.

[12] K. Otsuka and X. Ren, "Physical metallurgy of Ti-Ni-based shape memory alloys," *Progress in Materials Science*, vol. 50, no. 5, pp. 511–678, 2005.

[13] S.-Y. Jiang, Y.-N. Zhao, Y.-Q. Zhang, L. Hu, and Y.-L. Liang, "Effect of solution treatment and aging on microstructural evolution and mechanical behavior of NiTi shape memory alloy," *Transactions of Nonferrous Metals Society of China*, vol. 23, no. 12, pp. 3658–3667, 2013.

[14] J. I. Kim and S. Miyazaki, "Effect of nano-scaled precipitates on shape memory behavior of Ti-50.9 at.% Ni alloy," *Acta Materialia*, vol. 53, no. 17, pp. 4545–4554, 2005.

[15] A. R. Pelton, J. Dicello, and S. Miyazaki, "Optimisation of processing and properties of medical grade Nitinol wire," *Minimally Invasive Therapy & Allied Technologies*, vol. 9, no. 2, pp. 107–118, 2009.

[16] K. W. K. Yeung, K. M. C. Cheung, W. W. Lu, and C. Y. Chung, "Optimization of thermal treatment parameters to alter austenitic phase transition temperature of NiTi alloy for medical implant," *Materials Science and Engineering: A*, vol. 383, no. 2, pp. 213–218, 2004.

[17] M. F. Razali and A. S. Mahmud, "Gradient deformation behavior of NiTi alloy by ageing treatment," *Journal of Alloys and Compounds*, vol. 618, no. 5, pp. 182–186, 2015.

[18] M. R. Aboutalebi, M. Karimzadeh, M. T. Salehi, S. M. Abbasi, and M. Morakabati, "Influences of aging and thermomechanical treatments on the martensitic transformation and superelasticity of highly Ni-rich Ti-51.5 at.% Ni shape memory alloy," *Thermochimica Acta*, vol. 616, no. 20, pp. 14–19, 2015.

[19] D. Favier, Y. Liu, and L. Orgéas, "Influence of thermomechanical processing on the superelastic properties of a Ni-rich Nitinol shape memory alloy," *Materials Science and Engineering: A*, vol. 429, no. 1-2, pp. 130–136, 2006.

[20] X. Lu, G. Li, L. Liu, X. Zhu, and S. T. Tu, "Effect of ambient temperature on compressibility and recovery of NiTi shape memory alloys as static seals," *Advances in Mechanical Engineering*, vol. 9, no. 2, pp. 1–9, 2017.

[21] X. Wang, B. Xu, and Z. Yue, "Phase transformation behavior of pseudoelastic NiTi shape memory alloys under large strain," *Journal of Alloys and Compounds*, vol. 463, no. 1-2, pp. 417–422, 2008.

[22] B. Ben Fraj, A. Gahbiche, S. Zghal, and Z. Tourki, "On the influence of the heat treatment temperature on the superelastic compressive behavior of the Ni-rich NiTi shape memory alloy," *Journal of Materials Engineering and Performance*, vol. 26, no. 11, pp. 5660–5668, 2017.

[23] Y. Liu, J. V. Humbeeck, R. Stalmans, and L. Delaey, "Some aspects of the properties of NiTi shape memory alloy," *Journal of Alloys and Compounds*, vol. 247, no. 1-2, pp. 115–121, 1997.

[24] G. Fan, W. Chen, S. Yang, J. Zhu, X. Ren, and K. Otsuka, "Origin of abnormal multi-stage martensitic transformation behavior in aged Ni-rich Ti-Ni shape memory alloys," *Acta Materialia*, vol. 52, no. 14, pp. 4351–4362, 2004.

[25] S. Miyazaki, *Thermal and Stress Cycling Effects and Fatigue Properties of Ni-Ti Alloys*, pp. 394–413, Engineering Aspects of Shape Memory Alloys, London, UK, 1990.

[26] H. Mohamad, A. S. Mahmud, M. N. Nashrudin, and M. F. Razali, "Effect of ageing temperatures on pseudoelasticity of Ni-rich NiTi shape memory alloy," in *Proceedings of the 3rd International Conference on the Science and Engineering of Materials*, AIP Publishing LCC, Melville, NY, USA, May 2018.

[27] Z. Yuan, Z. Feng, and W. Miao, "High damping capacity of a binary TiNi shape memory alloy," *Materials Science Forum*, vol. 687, pp. 485–489, 2011.

[28] M. Karimzadeh, M. R. Aboutalebi, M. T. Salehi, S. M. Abbasi, and M. Morakabati, "Effects of thermomechanical treatments on the martensitic transformation and critical stress of Ti-50.2 at.% Ni alloy," *Journal of Alloys and Compounds*, vol. 637, pp. 171–177, 2015.